Weak beam control of two-dimensional multicolored transverse arrays in a quadratic nonlinear medium

Heping Zeng*, Jian Wu, Kun Wu, and Han Xu
Key Laboratory of Optical and Magnetic Resonance Spectroscopy, and Department of Physics, East China Normal University, Shanghai 200062, People's Republic of China

We demonstrate the generation and weak beam control of two-dimensional (2D) multicolored transverse arrays in a thick quadratic nonlinear medium pumped by two spatially overlapped and temporally synchronized femtosecond beams. Above relatively low input fundamental pulse intensities ($\sim$ 6.7 GW/cm^2), reproducible multiple filaments are induced by small ellipticity of one of input beams, and two-dimensional multicolored transverse arrays are launched as a result of multiple four-wave mixing between the induced multiple filaments and crossly coupled fundamental and second harmonic pulses. By seeding with weak second harmonic pulses, the two-dimensional arrays are suppressed into one-dimensional ones. The weak beam control is independent upon the relative phase of the second harmonic seed. This suggests a simple but robust phase-insensitive all-optical control to switch 2D array of strong beams with a weak seed beam, in contrast with the requisite of a strong beam to control a weak beam in the usual case of all-optical switching. Furthermore, the phase-insensitive control is of practical importance, since it provides an unusual coherent process without any necessities to determine the phase of the signal and match it to an appropriate phase of the control beam as normally required for usual all-optical switches.

PACS number(s): 42.65.Sf, 42.65.Tg, 03.50.De, 42.65.Jx.

Generation of multiple filaments and soliton-like waves during the propagation of intense wave packets is currently one of the most active areas in nonlinear optics. The form of multiple filaments can be considered as amplification of perturbations in the input beams or noise in the nonlinear optical systems [1–13]. In the absence of any external perturbations, the breakup of a low-noise input wave packet is triggered and ruled by deterministic wave-envelope modulation in spite of stochastic nature of the input noise [14]. Deterministic multiple filament patterns that are reproducible from shot to shot have been observed for elliptical input beams propagating in water [15]. Control of multiple filaments has been demonstrated for intense elliptical beams propagating in air by changing the input ellipticity [16]. Stable multiple quadratic solitons have been generated in a quadratic nonlinear medium due to the nature anisotropy of the medium or input beam asymmetry [17–19]. It has been shown that the quadratic solitons could be simply controlled by seeding a second harmonic (SH) beam [20].

On the other hand, one-dimensional multiple soliton-like waves could be generated due to the spatial modulational instability in a quadratic nonlinear medium [21]. However, the onset of 2D soliton-like waves required a quite high-intensity pump, which was obviously limited by the damage thresholds of the nonlinear materials. A recent experiment has demonstrated that 2D multicolored transverse arrays (MTAs) could be launched in a quadratic nonlinear medium at relatively low input fundamental-wave (FW) intensities [22], as a result of multiple four-wave mixing between the crossly coupled FW and SH pulses and the reproducible multiple filaments induced by the small input beam asymmetry. The observed 2D MTAs may find interesting applications in ultrafast photonics. For instance, a 2D array of all-optical switches can be developed if the 2D MTAs can be controlled with appropriate seeding pulses. As the 2D MTAs were caused by multiple four-wave-mixings involving the reproducible multiple filaments, which could be controlled by a weak SH seed [20], accordingly, a weak SH seed can be used to suppress 2D MTA patterns. In this letter, we demonstrate that 2D MTA patterns can be switched into 1D ones by using a weak SH seeding along one of FW input beam. The controlling process was verified to be independent upon the relative phase shift between the FW and the seeded SH pulses.

The experimental setup is sketched in Fig.1. A regeneratively amplified Ti:sapphire fs laser (Spectra-Physics, Spitfire) was used to produce fundamental pumping pulses (50 fs, 800 nm), which were split into an on-axis beam $\vec{k}_1$ and slightly off-axis beam $\vec{k}_2$. The on-axis $\vec{k}_1$ laser beam was focused by a spherical concave high-reflection mirror at a small fold angle, and the off-axis $\vec{k}_2$ fundamental beam was down-collimated with a concave high-reflection mirror and a lens. Both input beams were polarized perpendicular to $\vec{k}_1$ and $\vec{k}_2$, and were steered to cross inside a 4mm-thick β-barium borate (BBO II, type-I 29.18°-z cut) crystal at a variable angle (θ_p) with accurate synchronization and spatial cross-overlapping, and the BBO II crystal was placed 20 mm before the focus point of the $\vec{k}_1$ beam. The beam diameters of the pumping pulses were about 1.3 mm. The BBO II crystal was arranged so that the on-axis $\vec{k}_1$ beam fulfilled the type-I SH phase-matching condition.

In the presence of only the on-axis $\vec{k}_1$ beam, the FW and SH pulses were observed to break up spatially into

stable filaments [2–13]. This was caused by the on-axis beam ellipticity [15,16,19] due to the asymmetric focusing with concave high-reflection at a small fold angle. For example, at a fold angle of $\sim 12^{\circ}$, the on-axis $\vec{k}_1$ pump beam was focused into an elliptical beam of the spatial profile as $E(x,y) = F(x^2/a^2+y^2/b^2)$ with $e = b/a = 1.58$ on the input facet of the BBO II crystal. Within the crystal, quadratic nonlinearity brought about a stable spatial break of the input elliptical FW beam and the associated SH beam into two colored filaments along the minor axis [15,16,19]. The red filament showed a quite broad spectrum, while the spectrum of the blue one was relatively narrow. As shown in Fig.2(a), the inner blue filaments corresponded to the sum-frequency generation between the on-axis $\vec{k}_1$ pulses and the outer red filaments. As both the on-axis $\vec{k}_1$ and off-axis $\vec{k}_2$ beams were synchronously crossed the BBO II crystal, MTAs were observed at an observation screen perpendicular to $\vec{k}_1$. Figure 2(d) shows a typical MTA pattern observed with an intensity ratio $I_{\vec{k}_1}/I_{\vec{k}_2} = 17$ and cross angle θ_p=2.75°. The observed patterns consisted of red and blue arrays, denoted by R(n_r, m_r) and B(n_b, m_b), where R(n_r=0, m_r=0), R(n_r=1, m_r=0), and $R(n_r = \pm 1, m_r = 0)$ represent the $\vec{k}_1$ and $\vec{k}_2$ beams, and red multiple filaments, while $B(n_b = 0, m_b = \pm 1)$, $B(n_b = 0, m_b = 0)$, and $B(n_b = 1, m_b = 0)$ represent the blue multiple filaments, SH of the $\vec{k}_1$ beam, and frequency-summed pulses $\vec{k} = \vec{k}_1 + \vec{k}_2$, respectively. The onset of MTAs was critically dependent upon the pump intensity, which was measured to be consistent with the onset of multiple filaments. In principle, the observed MTAs were caused by multiple four-wave-mixings as follows. Four-wave mixing between $B(n_b = 0, m_b = \pm 1)$, $B(n_b = 0, m_b = 0)$, and $B(n_b = 1, m_b = 0)$ generated $B(n_b = 1, m_b = \pm 1)$, and further multiple four-wave-mixings generated $B(n_b, m_b)$ in the observed blue MTAs [22]. Similarly, the red patterns $R(n_r, m_r)$ were generated by multiple four-wave-mixings originated from $R(n_r = \pm 1, m_r = 0)$, R(n_r=0, m_r=0), and R(n_r=1, m_r=0) [22]. The generated reproducible multiple filaments were involved in the multi-step nonlinear couplings as novel beams.

In order to investigate the effect of SH seed on the generation of 2D MTAs, we used a straightforward experimental setup as follows. A 1mm-thick BBO crystal (BBO I, type-I 29.18°-z cut) was placed before the 4mm-thick BBO II crystal, which provided a weak seed SH generation of the on-axis FW beam. The energy ratio SH/FW of the on-axis beam before BBO II crystal was changed by rotating the BBO I crystal to vary the phase-matching condition. Figure 2 shows clearly the control of multiple filaments and the corresponding MTAs by varying the input SH seed. Both red and blue filaments were completely suppressed when the energy ratio SH/FW was increased up to 3.6%. Correspondingly, all the red and blue patterns $R(n_r \neq 0, m_r)$ and $B(n_b \neq 0, m_b)$ were completely suppressed as a result of complete suppression of multiple four-wave-mixings, and the 2D MTA patterns were switched to 1D one. Even under a complete suppression of red and blue multiple filaments, there still existed coplanar nonlinear couplings between the $\vec{k}_1$ and $\vec{k}_2$) beams, which generated beams within the plane ($\vec{k}_1$, $\vec{k}_2$).

To verify that the suppression of 2D MTAs was not originated from intensity decrease of the on-axis FW pulse, BBO I was rotated so that no SH pulses were generated and the on-axis FW pulses were attenuated by a variable attenuator. The threshold to launch multiple filaments and 2D MTAs was about 6.7 GW/cm^2. However, when the 2D MTA patterns were suppressed by seeding a weak SH pulse, the residual FW pulse intensity after BBO I was about 15.0 GW/cm^2. It clearly indicates that the suppression of the 2D MTAs is originated from the weak SH seed rather than intensity decrease of the FW pulse. A detailed dependence of the 2D MTAs upon the energy ratio SH/FW is plotted in Fig.3. The intensities of the 2D MTA patterns decrease monotonously with the increase of the energy ratio SH/FW. The blue patterns could be suppressed at a smaller SH seed than the red patterns. It is consistent with the fact that the inner blue filaments were generated by the frequency-summing of the on-axis FW beam and the outer red filaments. It is clear that the suppression of 2D MTA patterns was accompanied with the suppression of red and blue multiple filaments. This presents an experimental evidence that the formation of 2D patterns were originated from four-wave mixing between input beams and the induced multiple filaments.

To understand the intrinsic physics of the experimental observations, we performed numerical simulations. The real experimental situations can only be simulated by solving the (3+1)D equations for the slowly-varying envelopes of relevant electric fields, which involves a formidable computation task since multiple filament generation and fs pulse propagation in the quadratic nonlinear medium cannot be simulated by using cylindrical symmetry. Fortunately, it has been demonstrated that multiple filaments can be described successfully as a spatial breakup in the frame of spatial (CW) models in spite of the genuine spatiotemporal nature of the involved processes [23,24]. For the sake of simplicity, we neglect in our simulation the pulse properties of the coupled waves, such as the group-velocity mismatch, group-velocity dispersion, and etc., and adopt a simplified (CW) simulation by solving the coupled wave equations [18,20]

$$2ik_1\frac{\partial E_1}{\partial z} + \nabla_{\perp}^2 E_1 + \Gamma E_2 E_1^* e^{-i\Delta kz} = 0,$$

$$2ik_2\frac{\partial E_2}{\partial z} + \nabla_\perp^2 E_2 + 2\Gamma E_1^2 e^{i\Delta kz} = 0, \qquad (1)$$

where k_i(i=1,2) are the wave vectors of FW (E_1)and SH (E_2) pulses, and $\Delta k = 2k_1 - k_2$ is the wave vector mismatch. The parameter Γ is proportional to the effective second-order nonlinear coefficient d_{eff} (d_{eff} = 2.08 pm/v for BBO used here). $\nabla_\perp^2 = \partial^2/\partial_x^2 + \partial^2/\partial_y^2$ stands for the transverse diffraction. Although the adopted numerical model did not represent the experimental situations, the simplified (CW) simulations qualitatively reproduced the experimental observations with regard to the role of input asymmetry and SH seed in the generation of multiple filaments. Figure 5(a) shows that an additional pair of filament are generated when a small asymmetry is assumed in the input pulses (b/a=2.0). Then, by seeding a weak SH pulse (SH/FW=1.0 %), the wave break is completely suppressed and the filaments around the on-axis input beam disappear. As the generation of MTAs is closely related with multiple filaments, suppression of multiple filaments eventually leads to suppression of the MTA patterns out of the plane($\vec{k}_1$, $\vec{k}_2$), and thus a switch of MTAs patterns from 2D into 1D can be observed.

Interestingly, the switching of the MTA patterns from 2D to 1D is not dependent on the relative phase between the on-axis FW and the seeded SH pulses. In the experiments, as shown in Fig.1, the relative phase shift can be changed by tilting an inserted 1mm-thick CaF_2 plate. Due to the dispersion property of the plate, the pulses with different carrier frequencies undergo different effective optical lengths, which introduces a relative phase shift. As shown in Fig.5, as an example, the disappearance of the filaments and 2D MTA patterns out of the ($\vec{k}_1$, $\vec{k}_2$) plane is not affected as the relative phase shift was varied from 0 to 2π by tilting the inserted thin plate.

In summary, we have demonstrated a weak beam control of 2D MTAs. By seeding a weak SH pulse, 2D MTA patterns were switched to 1D ones, and the switching was independent upon the SH seed phase. This may lead to various intriguing applications in ultrafast information processing such as all-optical multi-switches, in which a weak beam controls an array of strong beams.

This work was supported in part by Key Project from Shanghai Science and Technology Commission (Grant 04dz14001), by National Key Project for Basic Research (Grant TG1999075204), and by National Natural Science Fund (Grant 60478011).

[1] M. Mlejnek, M. Kolesik, J. V. Moloney, and E. M. Wright, Phys. Rev. Lett. **83**, 2938 (1999).
[2] L. Bergé, S. Skupin, F. Lederer, G. Méjean, J.Yu, J. Kasparian, E. Salmon, J. Wolf, M. Rodriguez, L.Wöste, R. Bourayou, and R. Sauerbrey, Phys. Rev. Lett. **92**, 225002 (2004).
[3] G. Méjean, A. Couairon, M. Franco, B. Prade, and A. Mysyrowicz, Phys. Rev. Lett. **93**, 035003 (2004).
[4] S. A. Hosseini, Q. Luo, B. Ferland, W. Liu, S. L. Chin, O. G. Kosareva, N. A. Panov, N. Aközbek, and V. P. Kandidov, Phys, Rev. A **70**, 033802 (2004).
[5] O. G. Kosareva, V. P. Kandidov, A. Brodeur, C. Y. Chien, and S. L. Chin, Opt. Lett. **22**, 1332 (1997).
[6] N. Akozbek, A. Iwasaki, A. Becker, M. Scalora, S. L. Chin, and C. M. Bowden, Phys. Rev. Lett. **89**, 143901 (2002).
[7] L. Sudrie, A. Couairon, M. Franco, B. Lamouroux, B. Prade, S. Tzortzakis, and A. Mysyrowicz, Phys. Rev. Lett. **89**, 186601 (2002).
[8] S. Carrasco, S. Polyakov, H. Kim, L. Jankovic, G. Stegeman, J. Torres, L. Torner, M. Katz, and D. Eger, Phys. Rev. E **67**, 046616 (2003).
[9] H. Kim, L. Jankovic, G. Stegeman, S. Carrasco, L. Torner, D. Eger, and M. Katz, Opt. lett. **28**, 640 (2003).
[10] F. Courvoisier, V. Boutou, J. Kasparian, E. Salmon, G. Méjean, J. Yu, and J. Wolf, Appl. Phys. Lett. **83**, 213 (2003).
[11] A. Dubietis, E. Gaižauskas, G. Tamošauskas, and P. Di Trapani, Phys. Rev. Lett. **92**, 253903 (2004).
[12] P. K. Shukla and B. Eliasson, Phys. Rev. Lett. **92**, 073601 (2004).
[13] S. Skupin, L. Bergé, U. Peschel, and F. Lederer, Phys. Rev. Lett. **93**, 023901 (2004).
[14] D. Salerno, S. Minardi, J. Trull, A. Varanavicius, G. Tamosauskas, G. Valiulis, A. Dubietis, D. Caironi, S. Trillo, A. Piskarskas, and P. Di Trapani, Phys. Rev. Lett.**91**, 143905 (2003).
[15] A. Dubietis, G. Tamošauskas, G. Fibich, and B. Ilan, Opt. Lett. **26**, 1126 (2004).
[16] G. Fibich, S. Eisenmann, B. Ilan, and A. Ziggler, Opt. Lett. **29**, 1772 (2004).
[17] S. Polyakov, R. Malendevich, L. Jankovic, G. Stegeman, C. Bosshard, and P. Gunter, Opt. Lett. **27**, 1049 (2002).
[18] S. V. Polyakov and G. I. Stegeman, Phys. Rev. E **66**, 046622 (2002).
[19] S. Carrasco, S. Polyakov, H. Kim, L. Jankovic, G. I. Stegeman, J. P. Torres, L. Torner, M. Katz, and D. Eger, Phys. Rev. E **67**, 046616 (2003).
[20] S. Polyakov, H. Kim, L. Jankovic, G. Stegeman, and M. Katz, Opt. Lett. **28**, 1451 (2003).
[21] R. A. Fuerst, D. M. Baboiu, B. Lawrence, W. E. Torruellas, G. I. Stegeman, S. Trillo, and S. Wabnitz, Phys. Rev. Lett. **78**, 2756 (1997).
[22] H. Zeng, K. Wu, H. Xu, and J. Wu, (unpublished).
[23] P. Di Trapani, G. Valiulis, A. Piskarskas, O. Jedrkiewicz, J. Trull, C. Conti, and S. Trillo, Phys. Rev. Lett. **91**, 093904 (2003).
[24] H. Zeng, J. Wu, H. Xu, K. Wu, and E Wu, Phys. Rev. Lett. **92**, 143903 (2004).

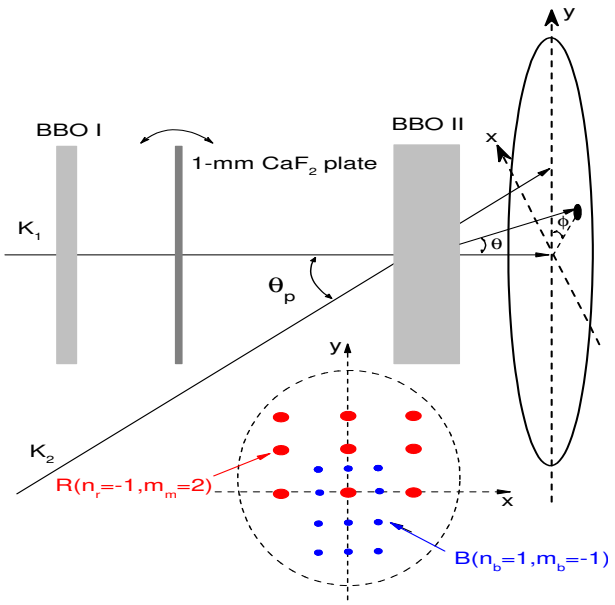

FIG. 1. Experimental scheme for the generation and control of 2D MTAs, and definition of 2D MTA patterns.

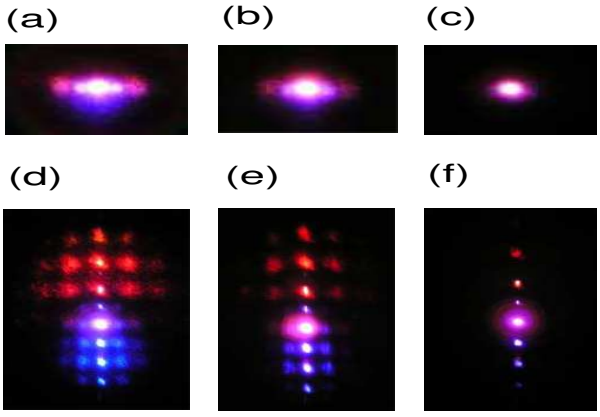

FIG. 2. MFs of the on-axis $\vec{k}_1$ beam (above) and the corresponding MTAs (below) under different SH/FW ratios of the on-axis beam $\vec{k}_1$. SH/FW=0% (a,d), 1.6% (b,e), and 3.6%(c,f).

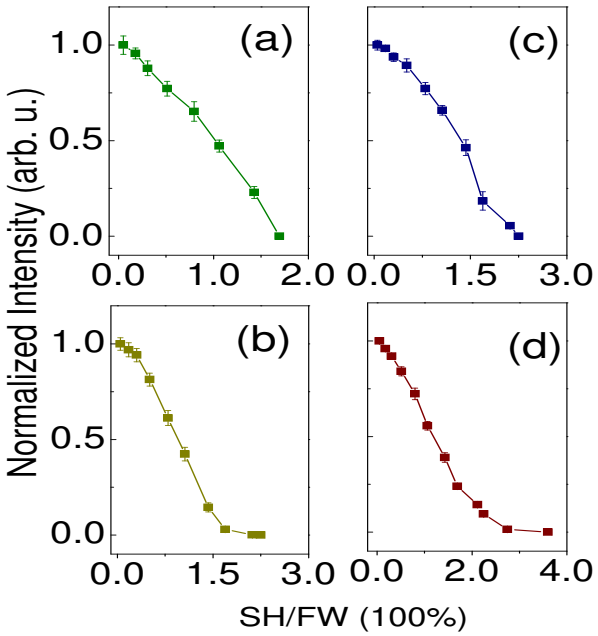

FIG. 3. Weak SH seed control of MTA patterns B(n_b=-1, m_b=-2) (a) and R(n_r=1, m_r=2) (b) in the presence of the off-axis pulses, and weak SH seed control of MF B(n_b=± 1, m_b=0) (c) and R(n_r=± 1, m_r=0) (d) in the absence of the off-axis pulses.

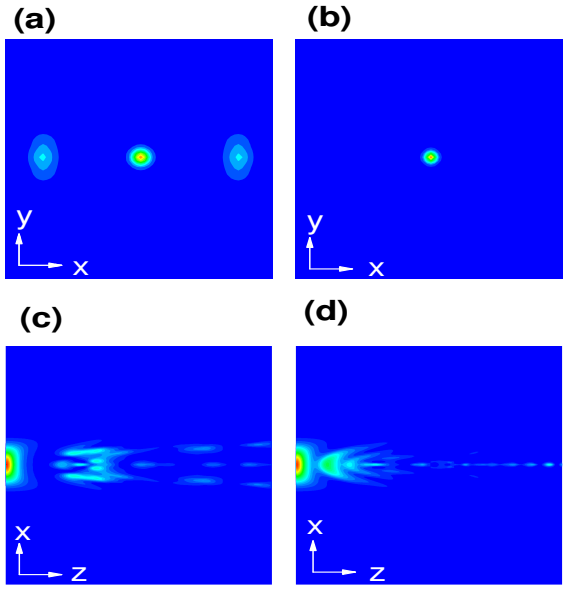

FIG. 4. CW simulations: FW intensity profiles at the output of the crystal (above) and along the propagation distance z (below) under different SH/FW ratios SH/FW=0% (a,c) and 1% (b,d).

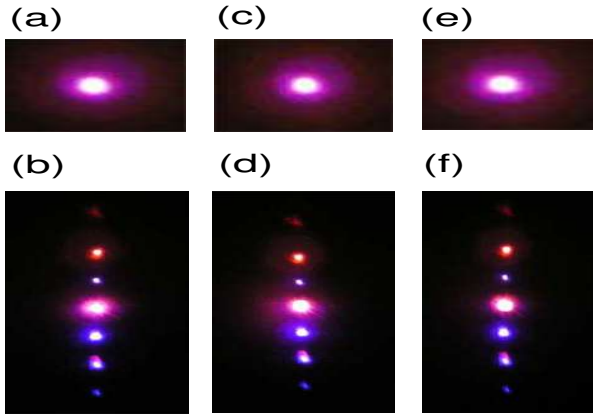

FIG. 5. MF (above) and MTA (below) patterns after the crystal with 3.6% SH pulse seeded under different phase shift between the SH and FW pulses as 0.26π (a,b), 1.05π (c,d), 2.36π (e,f).